Effects of Rolling-Induced residual stress on Subsequent Three-Point Bending Behaviour

Ravi Prakash Singh[1,2,[0000-0001-9055-3511]], Alison N. O'Connor[3,[0000-0002-8331-2901]] and Edward James Brambley [1,2,[0000-0002-5305-4892]].

[1] Mathematics Institute, University of Warwick, Coventry, CV4 7AL, UK
[2] WMG, University of Warwick, Coventry, CV4 7AL, UK
[3]Computer Science and Information Systems (CSIS), University of Limerick, Limerick, V94 T9PX, Ireland
E.J.Brambley@warwick.ac.uk

Abstract. Cold-rolled sheet has a complex through-thickness residual stress pattern, potentially of around two thirds the yield strength. In the current work, the influence of this residual stress on the subsequent three-point bending behaviour of a DC02 steel sheet is investigated, using a sequential finite element framework developed in ABAQUS. Three simulation cases are considered: rolling followed by bending, bending of an imported rolled geometry with residual stress removed, and bending of a virgin sheet. The rolling simulation reveals the anticipated oscillatory stress evolution within the roll gap leading to the formation of localized residual stress bands in the rolled sheet. Comparison of force–displacement curves for the subsequent bending operation shows the rolled sheet requiring a higher punch force, with both the imported rolled geometry and the virgin sheet requiring less. The results indicate that geometric distortion alone has limited to no influence on the bending response, accumulated plastic strain and strain hardening and rolling induced residual stress alters the bending resistance of the sheet. The ultimate aim of this study is to differentiate between hardening and residual stress effects, and to predict the three-point-bending behaviour indicative of the through-thickness residual stress pattern that could be verified experimentally.

Keywords: Plasticity, 3-point bending, cold rolling, residual stress.

1 Introduction

Rolling remains one of the most extensively employed metal forming processes in industrial manufacturing, with a significant proportion of ferrous and non-ferrous metals being processed through rolling operations before reaching their final usable forms being manufactured into products such as sheets, plates, rods and pipes (Ikumapayi et al., 2020). Owing to the large plastic strains involved during cold rolling, the material undergoes strain hardening accompanied by non-uniform through-thickness stress and strain development (Tarnovskii, 2013). Traditional slab-based analytical approaches are inadequate for accurately resolving through-thickness stress and strain evolution during rolling deformation. Consequently, advanced tests such as Digital Image Correlation (DIC) (Jacobs et al., 2022) and finite element simulations (Cawthorn et al., 2016; Yarita et al., 1985) have been employed to investigate the through-thickness behaviour of rolled sheets. More recently, asymptotic modelling of cold rolling carried out by Erfanian et al. (2025) revealed oscillatory through-thickness stress and velocity distributions during deformation. These oscillatory stress variations were further verified using high-precision careful finite element simulations incorporating 60 elements through the sheet thickness in ABAQUS by the same groups (Flanagan et al., 2025). It was concluded that these oscillatory patterns are physically meaningful and not merely numerical artefacts associated with modelling assumptions or material properties and play an important role in accurately predicting the curvature and residual stress evolution in rolled sheets (Guo & Xiao, 2026).

The non-uniform plastic deformation thorough the sheet thickness during cold rolling gives rise to residual stress fields, where a plane state of residual stress is developed with the dominant stress components occurring along the longitudinal (rolling direction) and transverse directions (Tadić et al., 2023). The presence of such residual stresses may result in strip flatness defects and distortion in rolled products (Tran et al., 2015). In addition, during subsequent loading, the superposition of applied and residual stresses can locally increase the stress state within the material and influence its mechanical response (Nakhoul et al., 2015). De Giorgi further reported that the through-thickness yield strength gradient introduced during cold rolling plays an important role in the evolution and redistribution of residual stresses under cyclic bending loading conditions (De Giorgi, 2011). Flanagan et al., (Flanagan et al., 2025) reported the development of distinct residual stress zones characterized by compressive longitudinal stresses near the sheet centre and tensile residual stresses close to the sheet surfaces. The study further observed localization of residual von Mises stresses within narrow bands, of the order of two thirds the yield stress, indicating a relationship between stress oscillations developed within the roll gap and the resulting residual stress distribution after deformation.

In the present work, we investigate the influence of rolling-induced residual stress fields on the subsequent deformation behaviour of sheet metals. The high-resolution rolling simulation framework developed by Flanagan et al. has been adopted as the benchmark rolling model, following which the rolled sheet is subjected to subsequent three-point bending deformation. The bending response of the rolled sheet is compared against that of a virgin sheet, and that of the as-rolled geometry with residual stresses removed, under identical loading conditions.

2 Methodology

2.1 Geometry, material and mesh details

The geometry for rolling and material parameters employed in the present study were adopted from the rolling simulation reported by Flanagan et al. (Flanagan et al., 2025). A two-dimensional plane-strain finite element framework was developed in ABAQUS 2025 to simulate the rolling and three-point bending behaviour of the sheet. The initial sheet dimensions were 150 mm in length and 4 mm in thickness. The rolling operation was performed using rigid analytical rollers of radius 30 mm, with a thickness reduction of 1 mm after rolling deformation. The subsequent three-point bending was set up to conform to ISO7438:2020 (International Organization for Standardization, 2020). An analytical rigid cylindrical punch and two rigid supports, all having a radius of 15 mm, were employed with a support span of 72 mm. The details of the rolling and three-point bending simulations, together with the material properties employed in the present study, are summarized in Table 1. The sheet material was modelled as elastic–plastic DC02 steel. The elastic response was characterized by a Young's modulus of 206.3 GPa and a Poisson's ratio of 0.3.The plastic behaviour was defined using experimentally obtained true stress–plastic strain data, with an initial yield stress of 477.2 MPa and an ultimate tensile strength of 650.25 MPa. The sheet was discretized using four-node reduced integration plane-strain elements (CPE4R). A refined mesh consisting of 60 elements through the sheet thickness was employed in order to capture the through-thickness stress and strain evolution during rolling and bending deformation (informed by (Flanagan et al., 2025). Surface-to-surface contact with hard normal contact behaviour was employed between the sheet and rigid tools, while Coulomb friction with a coefficient of 0.1 used.

Table 1: Details of simulation and materials in the current study:

Details of Rolling simulation		**Details of 3-point bending simulation**	
Radius of Roller	30 mm	Punch Radius	15 mm
Tangential Speed of Roller	1290 mm/sec	Distance between support	72 mm
Half thickness of sheet	2 mm	Punch displacement	2 mm
half-thickness reduction	0.5 mm	Velocity of punch	2 mm/sec
General simulation details		**Material Details**	
Step-type	Static, general	Yield Stress	477.2 MPa
Amplitude curve	Instantaneous	Ultimate tensile stress	650.25 MPa
Contact discretization	Surface to surface	Modulus of Elasticity	206.3 GPa
No of through thickness elements	60	Poisson's ratio	0.3
Type of sheet elements	CPE4R		

2.2 Description of simulation cases

Simulation 1 (S1): Rolling followed by three-point bending

Simulation 1 (S1), shown in figure 1(a,b), represents the sequential simulation in which the sheet is first cold rolled and then subjected to three-point bending to understand the effect of rolling induced residual stresses and accumulated plastic strains on the forming behaviour of the sheet. The analysis was carried out using multiple static general steps with geometric nonlinearity (NLGEOM) enabled. In the first step, (bite) the upper and lower rollers were moved towards the sheet using vertical velocity boundary conditions of −0.5 mm/s and +0.5 mm/s, respectively, to establish contact with the sheet. In the subsequent roll step, the vertical motion of the rollers was constrained and equal but opposite angular velocity boundary conditions were applied to the roller reference points. The upper roller was assigned an angular velocity of +5 rad/s, while the lower roller was assigned −5 rad/s, producing the rolling deformation. After completion of rolling, the roller rotation was stopped and the roller–sheet contact interactions were removed. The subsequent three-point bending simulation was performed within the same ABAQUS analysis, allowing the deformed geometry together with the residual stress field, equivalent plastic strain, and strain-hardening history to be directly transferred to the bending stage. Before the punch displacement was applied, the bending tools were positioned to establish initial contact with the sheet. Since the rolling and bending analyses were carried out using the same implicit ABAQUS/Standard solver, static equilibrium was satisfied at the end of each converged analysis step. Consequently, the residual stress field after roller removal was the equilibrated residual stress state that served as the initial condition for the subsequent bending simulation.

In the Bending step, three-point bending was imposed by applying a downward velocity of −2 mm/s to the central punch reference point, giving a total punch displacement of 2 mm. The supports were constrained during this stage, and the punch reaction force and displacement were extracted from the punch reference point. Finally, in the Relax step, the punch was unloaded, allowing the sheet to relax elastically.

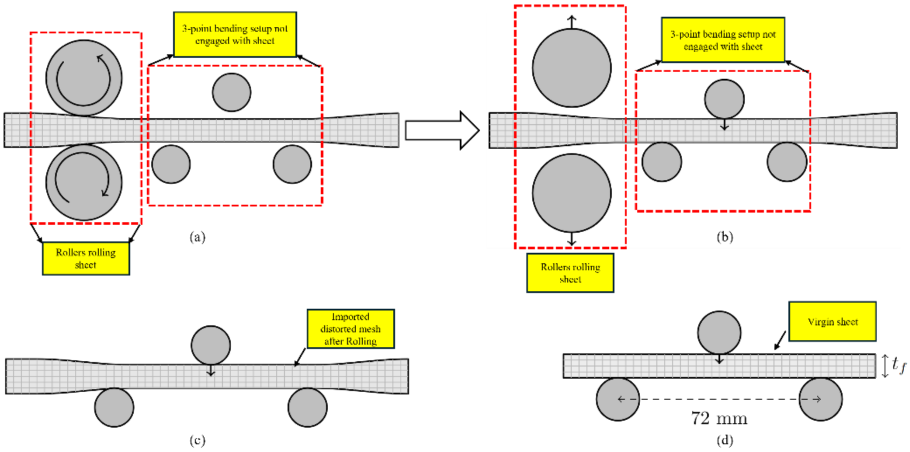

Figure 1: Schematic representation of the simulation sequence used for analyzing the effect of rolling-induced deformation history on subsequent three-point bending behaviour. (a) Rolling operation showing the sheet engaged between the rotating rollers while the three-point bending setup remains disengaged. (b) Transfer of the rolled sheet into the bending configuration after completion of rolling. (c) Imported distorted mesh after rolling deformation used as the initial geometry for bending analysis. (d) Reference virgin sheet geometry used for comparison with the rolled configuration prior to three-point bending.

Simulation 2 (S2): Three point bending of imported rolled geometry

Simulation 2 (S2), illustrated in Figure 1(c), corresponds to the three-point bending simulation performed on the imported rolled sheet geometry without transfer of the rolling-induced residual stress and accumulated plastic strain fields. In this case, only the geometrically distorted rolled configuration obtained after rolling was transferred into the bending simulation in order to isolate the influence of geometric distortion on the subsequent bending response of the sheet. The bending simulation consisted of Bending and Relax steps, where the punch displacement and unloading conditions were applied identically to S1.

Simulation 3 (S3): Three-point bending of virgin sheet

Simulation 3 (S3), illustrated in Figure 1(d), corresponds to the three-point bending simulation performed on a virgin sheet without any prior rolling deformation history. In this case, the sheet geometry and material properties were considered identical to those used in the rolling simulation of S1, while no rolling-induced residual stress, accumulated plastic strain, or geometric distortion was transferred to the bending model. The bending simulation consisted of Bending and Relax steps similar to those employed in S1 and S2.

3 Results and discussion

3.1 Residual stress in sheet post rolling

Figure 2(a) shows the oscillatory shear stress distribution developed within the roll gap during rolling deformation. Similar oscillatory stress evolution during rolling was reported by Erfanian et al.(Erfanian et al., 2025) using and Flanagan et al. (Flanagan et al., 2025) using ultra fine FEA simulation (30 TT elements for half thickness of 2 mm) demonstrated that that the rolling process develops through-thickness stress oscillations within the deformation zone due to the complex plastic flow occurring inside the roll gap. The oscillatory pattern shown in figure 2(a) for full sheet confirms that the mesh density used in the study is sufficient to resolve the stresses observed during rolling.

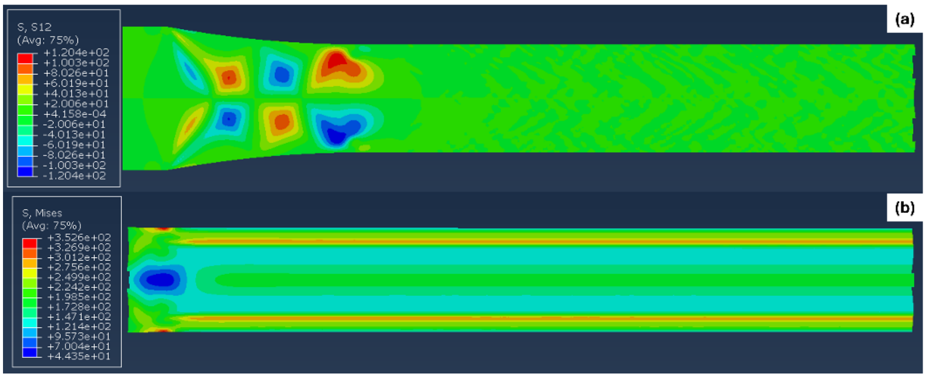

Figure 2: Distribution of stress component σ_{12} and von Mises stress during and post rolling, respectively: (a) oscillatory shear stress (σ_{12}) distribution in the sheet during the rolling process;

and (b) von Mises stress distribution illustrating the through-length stress evolution induced by rolling deformation. The contours highlight the formation of residual stress bands originating from sheet rolling.

Flanagan et al. (2025) further observed that the residual von Mises stress after unloading accumulated within narrow horizontal bands located between the sheet surface and the sheet centerline, with the central region of the sheet experiencing longitudinal compression and the outer regions remaining under longitudinal tension. Consistent with these observations, the present simulations also exhibit pronounced residual stress band formation after rolling, as shown in Figure 2(b). To quantify this behaviour, the corresponding through-thickness residual von Mises stress profiles extracted at three longitudinal locations (Paths 1–3) are presented in Figure 3(a,b). The three profiles overlap almost completely, indicating that the residual stress field is essentially invariant along the sheet when sufficiently far from the rollers. This observation is consistent with the expectation from Saint-Venant's principle that the local effects of the roll contact diminish rapidly with increasing distance from the loading region and are negligible only a few sheet thicknesses away. The profiles clearly exhibit two near-but-not-at-surface peaks of approximately 295 MPa confined in the narrow horizontal bands.

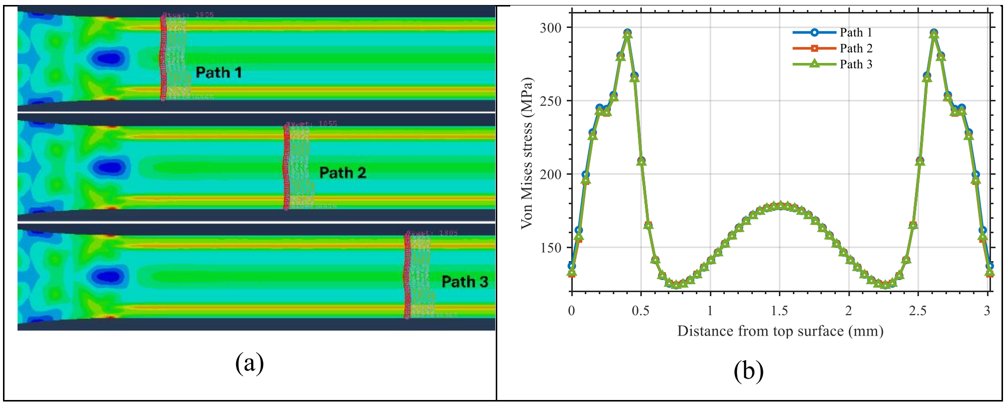

*Figure 3: Von Mises stress after rolling **(a)** Residual stress contours showing the locations of the three through-thickness extraction paths (Paths 1–3) at increasing distances downstream of the roll bite. **(b)** Through-thickness residual von Mises stress profiles corresponding to Paths 1–3.*

The spatial localization and magnitude of residual stress within these bands are likely to be strongly influenced by the nature of the oscillatory stress patterns developed within the roll gap. Since the characteristics of these oscillations depend on the roll-gap aspect ratio and rolling parameters, the resulting residual stress distribution after unloading is also expected to be highly sensitive to the rolling configuration. Such residual stress fields, together with the accumulated plastic strain developed during rolling, are expected to influence the subsequent bending behaviour of the sheet, which is the central focus of current research and related future studies. To assess this, the punch force response obtained from the three simulation cases described in Section 2.2 is first examined and compared.

3.2 Force-displacement response

Figure 3 shows the force–displacement response obtained for the three point bending portion of the three simulation cases. All configurations exhibit the expected initially linear response indicating elastic bending behaviour. Beyond this stage, nonlinear behaviour is observed due plastic deformation. The S1 configuration ultimately requires higher punch forces compared to S2 and S3, reaching a maximum punch force of approximately 85 N, whereas S2 and S3 exhibit almost identical behaviour with peak forces of nearly 74 N. The similarity between S2 and S3 indicates that the geometrical distortion introduced during rolling has limited influence on the subsequent bending response.

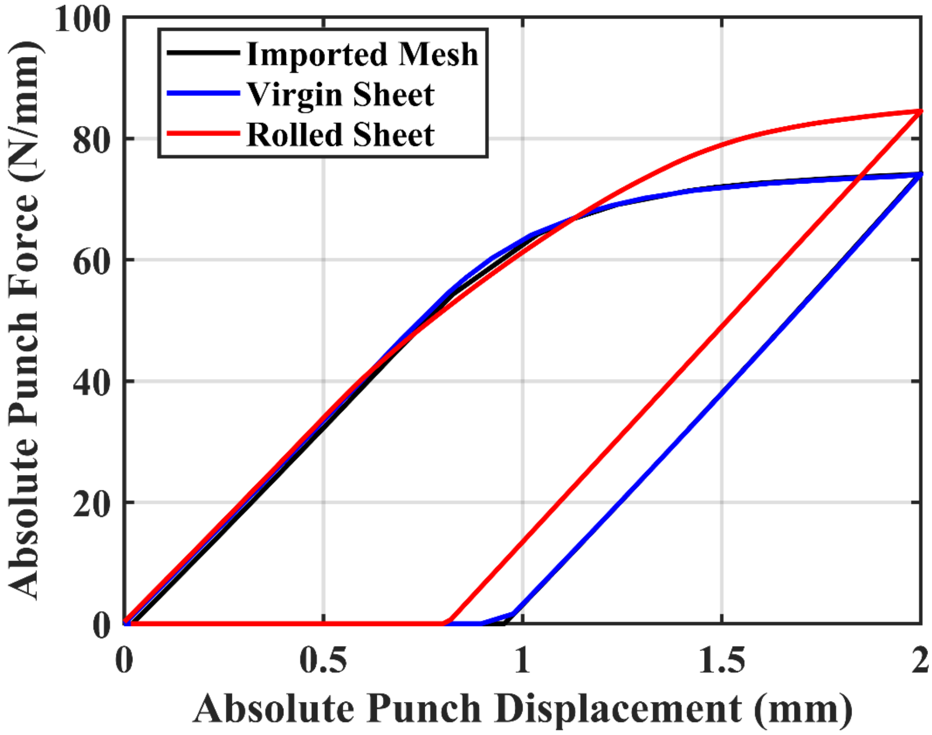

Figure 4: Comparison of the absolute punch force–displacement response obtained during three-point bending for the virgin sheet, rolled sheet, and imported mesh conditions. The results show the influence of prior rolling deformation and residual stress history on the bending response, with the rolled sheet exhibiting higher force requirements and altered unloading behaviour compared with the virgin sheet configuration.

The substantially higher force response observed in S1 is indicative of rolling-induced hardening. However, note that S1 actually shows lower force for a given displacement than S2 and S3 for punch displacements of around 0.6-1.1mm, well into the plastic deformation region. This is indicative of the residual stresses in the rolled sheet, which are a substantial fraction of the yield stress. These residual stresses initially aid the plastic deformation and make the material appear softer, even though it is clear from the subsequent deformation that it is in fact substantially harder. This behaviour cannot be attributed to the geometric change in the material, as samples S2 and S3 show the geometric differences have a minimal effect. Therefore, this behaviour suggests that the dominant mechanism governing the subsequent forming of cold-rolled sheets involves both the expected hardening and the through-thickness residual stress distribution.

4. Conclusions

The present study investigated the influence of rolling-induced deformation history on the subsequent three-point bending behaviour of a DC02 steel using ABAQUS simulation. The role of rolling-induced residual stresses, accumulated plastic strain, and geometric distortion on the punch force response during bending were investigated. Initial simulations of the rolling process showed the expected oscillatory stress pattern in the roll gap and the associated through-thickness variation of residual stresses (Flanagan et al., 2025), indicating sufficient through-thickness resolution was used.

The elevated forming force (85 N) during 3 point bending in S1 compared to imported rolled geometry S2 and virgin sheet S3 (with approximately 74 N for both) can be attributed to two factors: (a) the residual stress field developed post rolling; and (b) hardening due to accumulated plastic strain during rolling. Work is in progress to separate these effects. The sole effect of residual stress on 3 point bending will be studied by running simulation for non hardening material using elastic-perfectly plastic material model with the yield stress of the imported rolled geometry in S2 to be the average through-thickness yield stress attained by the rolled sheet after rolling; similar simulation were also described by Flanagan et al (2025).

The close agreement between S2 and S3 demonstrates that the geometric distortion introduced during rolling has a negligible influence on the subsequent bending response; i.e. that hardening and residual stress should be sufficient to predict subsequent forming behaviour. Future work in this area is to isolate these effects by using non hardening material models for rolling so that only residual stresses can be transferred in S2. The current results suggest that the complete bending response, including the shape of the punch force–displacement curve, the unloading behaviour, springback, and the final curvature, is likely to be sensitive to the underlying residual stress distribution. Future studies will quantify the individual sensitivity of these measurable responses and how they may be used to develop a simplified predictive model for residual stress prediction.

Ultimately, it would be advantageous if a simplified predictive model of the effect of rolling on residual stress, and its subsequent effect on subsequent forming, could be developed. Such a model could involve similar asymptotic modelling to that of Erfanian et al. (2025), and a suitably quick-to-compute model might be usable in an inverse problem to enable the use of an experimental three-point bending test to infer information about the likely through-thickness residual stress distribution.

References

Cawthorn, C. J., Minton, J. J., & Brambley, E. J. (2016). Asymptotic analysis of cold sandwich rolling. *International Journal of Mechanical Sciences*, *106*, 184–193. https://doi.org/10.1016/j.ijmecsci.2015.12.012

De Giorgi, M. (2011). Residual stress evolution in cold-rolled steels. *International Journal of Fatigue*, *33*(3), 507–512. https://doi.org/10.1016/j.ijfatigue.2010.10.006

Dieter, G. E. and B. D. and others. (1976). *Mechanical metallurgy* (Vol. 3). McGraw-hill New York.

Erfanian, M., Brambley, E. J., Flanagan, F., O'Kiely, D., & O'Connor, A. N. (2025). Through-thickness modelling of metal rolling using multiple-scales asymptotics. *European Journal of Mechanics - A/Solids*, *113*, 105712. https://doi.org/10.1016/j.euromechsol.2025.105712

Flanagan, F., O'Connor, A. N., Erfanian, M., Music, O., Brambley, E. J., & O'Kiely, D. (2025). Through-thickness resolution, stress oscillations and residual stress in cold rolling. *European Journal of Mechanics - A/Solids*, *114*, 105761. https://doi.org/10.1016/j.euromechsol.2025.105761

Guo, Y., & Xiao, H. (2026). Investigation of rolling deformation oscillations and the bending mechanism in asymmetric rolling. *Journal of Materials Research and Technology*, *40*, 3543–3554. https://doi.org/10.1016/j.jmrt.2025.12.319

Ikumapayi, O. M., Akinlabi, E. T., Onu, P., & Abolusoro, O. P. (2020). Rolling operation in metal forming: Process and principles – A brief study. *Materials Today: Proceedings*, *26*, 1644–1649. https://doi.org/10.1016/j.matpr.2020.02.343

International Organization for Standardization. (2020). *Metallic materials—Bend test ISO 7438:2020*.

Jacobs, L. J. M., Dam, K. N. H. van, Wentink, D. J., Rooij, M. B. de, Lugt, J. van der, Schipper, D. J., & Hoefnagels, J. P. M. (2022). Effect of asymmetric material entrance on lubrication in cold rolling. *Tribology International*, *175*, 107810. https://doi.org/10.1016/j.triboint.2022.107810

Nakhoul, R., Montmitonnet, P., & Potier-Ferry, M. (2015). Multi-scale method for modeling thin sheet buckling under residual stresses in the context of strip rolling. *International Journal of Solids and Structures*, *66*, 62–76. https://doi.org/10.1016/j.ijsolstr.2015.03.028

Tadić, N., Mišović, M., & Radović, Ž. (2023). An analysis of longitudinal residual stresses in EN AW-5083 alloy strips as a function of cold-rolling process parameters. *Journal of the Mechanical Behavior of Materials*, *32*(1). https://doi.org/10.1515/jmbm-2022-0297

Tarnovskii, I. Y. and P. A. and L. V. (2013). *Deformation of metals during rolling*. Elsevier.

Tran, D. C., Tardif, N., & Limam, A. (2015). Experimental and numerical modeling of flatness defects in strip cold rolling. *International Journal of Solids and Structures*, *69–70*, 343–349. https://doi.org/10.1016/j.ijsolstr.2015.05.017

Yarita, I., Mallett, R. L., & Lee, E. H. (1985). Stress and deformation analysis of plane-strain rolling process. *Steel Research*, *56*(5), 255–259. https://doi.org/10.1002/srin.198500631